Spin and lattice effects in the Kondo lattice model

M. Gulacsi,[1] A. Bussmann-Holder,[2] and A. R. Bishop[3]
[1]*Department of Theoretical Physics, Institute of Advanced Studies, The Australian National University, Canberra ACT 0200, Australia*
[2]*Max-Planck-Institut für Festkörperforschung, Heisenbergstrasse 1, 70569 Stuttgart, Germany*
[3]*Theoretical Division, Los Alamos National Laboratory, Los Alamos, New Mexico 87545, USA*
(Received 24 February 2004; revised manuscript received 25 February 2005; published 21 June 2005)

The magnetic properties of a system of coexisting localized spins and conduction electrons are investigated within an extended version of the one-dimensional Kondo lattice model in which effects stemming from the electron-lattice and on-site Coulomb interactions are explicitly included. After bosonizing the conduction electrons, is it observed that intrinsic inhomogeneities with the statistical scaling properties of a Griffiths phase appear and determine the spin structure of the localized impurities. The appearance of the inhomogeneities is enhanced by appropriate phonons and acts destructively on the spin ordering. The inhomogeneities appear on well-defined length scales and can be compared to the formation of intrinsic mesoscopic metastable patterns, which are found in two-fluid phenomenologies.

DOI: 10.1103/PhysRevB.71.214415 PACS number(s): 75.20.Hr, 71.27.+a, 71.28.+d

I. INTRODUCTION

The interplay of spin, charge, and lattice degrees of freedom has been investigated intensively in many transition metal oxides and especially in perovskite manganites, which have recently attracted new interest because of the discovery of colossal magnetoresistance (CMR). The initial understanding of the properties of manganites was based on the double-exchange mechanism within a Kondo lattice.[1] However, neutron-scattering[2] and electron-diffraction[3] experiments have revealed the simultaneous presence of charge and spin superstructures, which makes these early theoretical approaches incomplete.

The existence of charge, lattice, and spin modulations with a doping-dependent wave vector in $La_{2-x}Sr_xNiO_4$,[2,3] or the presence of charge ordering at half filling in $Nd_{0.5}Sr_{0.5}MnO_3$ (Ref. 4) and similar compounds, such as $Pr_{0.5}Ca_{0.5}MnO_3$,[5–8] all suggest that the theoretical understanding has to be extended to account for effects stemming from the lattice in order to understand the doping-dependent phase diagram and the richness of phases that are obtained. Similarly, in electron-doped charge-ordered manganites $La_{1-x}Ca_xMnO_3$ charge, orbital, and magnetic ordering has been observed.[9] Several experiments also confirmed this behavior in other compounds.[10–12] Charge ordering has also been found for other doping systems as in $Bi_{1-x}Ca_xMnO_3$ (Ref. 10) and in $La_{1-x}Ca_xMnO_3$ (doped with P_r)[12] for $x \geqslant 1/2$.

Because of these complex behaviors, manganese oxides have been intensively studied during the last few years. Since realistic models of these perovskites is impossible to solve completely, different approximation schemes have been introduced to account for the individual properties of their rich phase diagram. Typically, the electronic degrees of freedom are described by a Kondo lattice model (KLM), which in the strong Hund coupling limit reduces to the Zener[13] double-exchange Hamiltonian. Early theories,[1] proposed to explain the physics of CMR materials, have focused primarily on this model. As the previously noted experimental findings show, all the approaches based entirely on the phenomenon of double exchange are incomplete.[14] Understanding the complex phase diagram of the perovskites can be resolved by including additional physics in the Kondo lattice, in the form of electron-phonon coupling[14] originating from a Jahn-Teller splitting of the Mn^{3+} ion. Consequently, our first goal here is to understand the lattice effects in the KLM by including explicitly the interaction with the lattice degrees of freedom.

A further consequence of the strong Hund coupling is that three localized t_{2g}^3 orbitals of the Mn^{4+} ions will be aligned, giving rise to a $S=3/2$ localized spin. As most of the recent approaches to CMR are based on Monte Carlo simulations of one-dimensional models,[15] it has been argued that for finite temperatures a classical spin represents a reasonable approximation. However, this may not be the best approach, as the quantum fluctuations are the strongest in one dimension. Hence, our second goal here is to develop a bosonization approach that solves the full quantum spin KLM in one dimension. For completeness we will allow for both ferro- and antiferromagnetic coupling in the KLM. In CMR materials where the coupling is ferromagnetic, it is obvious that double exchange dominates. We will show in Sec. II that this is also the case for antiferromagnetic coupling, as in, e.g., heavy fermion compounds.[16]

The paper is organized as follows: in Sec. II we investigate the presence of double-exchange ferromagnetism in both $J<0$ and $J>0$ cases. Section III contains a description of our starting Hamiltonian. Section IV contains the details of the bosonized solution. Section V is devoted to a comprehensive description of the localized spin ordering. In Sec. VI the obtained phase diagram is analyzed in detail. Section VII contains the conclusions.

II. DOUBLE EXCHANGE

In order to gain a more transparent understanding of the double-exchange interaction we investigate first the case of two sites and one conduction electron, as was done by Anderson and Hasegawa, and de Gennes.[17] For simplicity, the localized spin is taken here to be $1/2$, as this will not effect the conclusions of this section.[17] In the case of ferro-

magnetic coupling ($J<0$) the ground-state energy is $E_{0,J<0}=-|J|/4-t$ with wave function $|\psi_0\rangle_{J<0}\equiv|\psi_{\mathrm{DE}}\rangle_{J<0,z}=|\Uparrow_z\uparrow_z,\Uparrow_z 0\rangle+|\Uparrow_z 0,\Uparrow_z\uparrow_z\rangle$, where $\Uparrow_z$ and $\uparrow_z$ refers to the z component of the impurity and conduction electron spins, respectively. As can be seen, ferromagnetism arises here via an Ising-type coupling, which allows for description of the ground state within a simple semiclassical approximation.[17]

For $J>0$ the situation is completely changed because of the singlet formation of localized and conduction electron spins. Because of this Kondo singlet formation, which is absent for the $J<0$ case, double exchange is often ignored in the discussions of the $J>0$ KLM. This case has usually been discussed in terms of the competition between Kondo singlet formation and the Ruderman-Kittel-Kasuya-Yosida (RKKY) interaction. For a half-filled band, this point of view appears to be sufficient. However for a partially filled conduction band an overwhelming amount of numerical data[18–21] proves that ferromagnetism appears for stronger coupling.

This cannot be explained in terms of RKKY, which operates at weak coupling, nor in terms of Kondo singlets, since they are nonmagnetic. The missing element is double-exchange ordering[22] because of an excess of localized spins over conduction electrons. Double exchange requires only that the number of conduction electrons is less than the number of localized spins. It operates in any dimension, for any sign of the coupling J and for any magnitude S_j^2 of the localized spins.[17] The double-exchange interaction is specific to the Kondo lattice and absent in single- or dilute-impurity systems in which the situation is reversed and the electrons greatly outnumber the localized spins.

Double-exchange is conceptually a very simple interaction: each electron has, on average, more than one localized spin to screen and, consequently, hops between several adjacent spins gaining screening energy at each site, together with a gain in kinetic energy. Since hopping is energetically most favorable for electrons that preserve their spin as they hop (called coherent hopping), this tends to align the underlying localized spins.[17]

For two sites, this causes a mixing of the total spin and an enhancement of the Hilbert space, where now 16 elements have to be considered. The ground-state energy is given by $E_{0,J>0}=-J/4-\sqrt{J^2+2Jt+4t^2}/2$ with wave functions $|\psi_0\rangle_{J>0}\propto|\psi_{\mathrm{KS}}\rangle_z+[1/(J/4-E_{0,J>0})]\{|\Uparrow_z\downarrow_z,\Uparrow_z 0\rangle+|\Uparrow_z 0,\Uparrow_z\downarrow_z\rangle-|\Uparrow_z\uparrow_z,\Downarrow_z 0\rangle-|\Downarrow_z 0,\Uparrow_z\uparrow_z\rangle\}$, where the Kondo singlet $|\psi_{\mathrm{KS}}\rangle_z$ states are $|\Uparrow_z\downarrow_z,\Uparrow_z,0\rangle-|\Downarrow_z\uparrow_z,\Uparrow_z 0\rangle+|\Uparrow_z 0,\Uparrow_z\downarrow_z\rangle-|\Uparrow_z 0,\Downarrow_z\uparrow_z\rangle$. $|\psi_0\rangle_{J>0}$ involves six basis elements (the degeneracy is partially lifted by conduction electron hopping) and hence falls outside the four dimensional space needed to establish double exchange for $J<0$.

In order to invoke double exchange as well, all three spin directions x, y, and z, have to be considered: $|\psi_0\rangle_{J>0}\propto[1-1/(J/4-E_{0,J>0})]|\psi_{\mathrm{KS}}\rangle_z+[1/(J/4-E_{0,J>0})]\{|\psi_{\mathrm{DE}}\rangle_{J>0,x}+|\psi_{\mathrm{DE}}\rangle_{J>0,y}+|\psi_{\mathrm{DE}}\rangle_{J>0,z}\}$, where $|\psi_{\mathrm{DE}}\rangle_{J>0,\alpha=x\ \mathrm{or}\ y}=\{|\Uparrow_\alpha\downarrow_\alpha,\Uparrow_\alpha 0\rangle+|\Uparrow_\alpha 0,\Uparrow_\alpha\downarrow_\alpha\rangle+|\Downarrow_\alpha\uparrow_\alpha,\Downarrow_\alpha 0\rangle+|\Downarrow_\alpha 0,\Downarrow_\alpha\uparrow_\alpha\rangle\}/\sqrt{2}$ and $|\psi_{\mathrm{DE}}\rangle_{J>0,\alpha=z}=|\Uparrow_z\downarrow_z,\Uparrow_z 0\rangle+|\Uparrow_z 0,\Uparrow_z\downarrow_z\rangle$. In spite of this extra complication, it is apparent from the above that also for $J>0$, ferromagnetism appears.

We show in Sec. V that coherent conduction electron hopping over a characteristic length λ may be incorporated into a bosonization description which keeps the electrons finitely delocalized. At lengths beyond λ, the electrons are described by collective density fluctuations, common to one-dimensional Fermi systems. The electrons remain finitely delocalized over shorter lengths and describe coherent hopping over several adjacent sites. This tends to align the underlying localized spins at stronger coupling. λ measures the effective range of the double-exchange interaction, and hence is proportional to the width of the magnetic polarons.

III. THE MODEL

The KLM considers the coupling between a half-filled narrow band (localized d or f) and conduction electrons. Even though studied intensively for the last two decades, the understanding of the KLM remains incomplete. Only in one dimension have numerical simulations[18–21] and bosonization techniques[22,23] been carried through to admit predictions about the phase diagram of the KLM. However, of special relevance to CMR materials[24] is the case where the KLM is extended to account for contributions stemming from the phonons. In particular, the small doping regime of these systems, which are ferromagnetic at low temperatures, seems to be appropriate for modelling within the KLM argumented by interactions with the lattice. In the following we present bosonized solutions of the KLM where on-site Coulomb and specific phonon contributions are explicitly included. This "extended" KLM model allows spin-and magnetoelastic-polaron formation, which we believe are of major importance in understanding these complex materials.

The Hamiltonian of the KLM in the presence of on-site Coulomb interaction reads

$$H_{\mathrm{KLM+U}}=-t\sum_{j,\sigma}(c_{j,\sigma}^{\dagger}c_{j+1,\sigma}+\mathrm{H.c.})+J\sum_j \mathbf{S}_{\mathrm{d},j}\cdot\mathbf{S}_{\mathrm{c},j}+U\sum_j n_{j,\uparrow}n_{j,\downarrow}, \tag{1}$$

where $t>0$ is the conduction electron hopping integral, $\mathbf{S}_{\mathrm{d},j}=\frac{1}{2}\Sigma_{\sigma,\sigma'}c_{\mathrm{d},j,\sigma}^{\dagger}\boldsymbol{\sigma}_{\sigma,\sigma'}c_{\mathrm{d},j,\sigma'}$, $\mathbf{S}_{c,j}=\frac{1}{2}\Sigma_{\sigma,\sigma'}c_{j,\sigma}^{\dagger}\boldsymbol{\sigma}_{\sigma,\sigma'}c_{j,\sigma'}$ and $\boldsymbol{\sigma}$ are the Pauli spin matrices. Fermi operators $c_{j,\sigma},c_{j,\sigma}^{\dagger}$ with subscript d refer to localized d-spins, whereas those not indexed refer to the conduction electrons. The on-site Coulomb repulsion is given by the Hubbard term proportional to U. In the CMR materials, the localized states are represented by the threefold degenerate Mn t_{2g}^3 d electrons with total spin $\frac{3}{2}$. However, for reasons of transparency, the localized spin is approximated here by spin $\frac{1}{2}$. This choice will not effect the results of the bosonization presented in Sec. IV, as only the conduction electrons will be bosonized. Accordingly, the properties of the model will be qualitatively independent of the magnitude of the localized spins, i.e., the basic features of the phase diagram for the three dimensional case appear in one dimensions as well.[25,26]

In the following the Kondo coupling J is measured in units of the hopping t and both cases, antiferromagnetic ($J>0$) and ferromagnetic ($J<0$) couplings, will be considered. The conduction band filling is given by $n=N_c/N<1$, where N is the number of lattice sites and N_c is the number of

conduction electrons. In order to understand the broad properties of CMR materials, we also allow for the number of impurity spins N_d to vary in such a way that $N_d/N<1$. In this way, doped or dilute Kondo lattice systems can also be studied. It will be shown that a dilute Kondo lattice system is dominated by short-range antiferromagnetic correlations.

In one dimension, the electron-phonon coupling can either be of intersite [Su-Schrieffer-Heeger (SSH)[27]] or on-site (Holstein[28]) character. The models we study assumes a dispersionless phonon mode with frequency ω. The neglect of the dispersion of bare phonons is not essential since it is absent in the Holstein model and the acoustic phonons are decoupled from the low-energy electronic spectrum in the continuum limit of the SSH model.[29] In this approximation the Holstein coupling to dispersionless phonons has the following form:

$$H_{\text{Holstein}} = \sum_i \left(\beta q_i n_{ci} + \frac{K}{2} q_i^2 + \frac{1}{2M} p_i^2 \right), \tag{2}$$

with the conduction electron density n_{ci} at site i, the lattice displacement q_i, its conjugate momentum p_i, the electron-phonon coupling strength β, the spring constant K, and the ionic mass M. Within the SSH model the coupling to phonons is modified to

$$H_{\text{SSH}} = \sum_i \left[\sum_\sigma \alpha_\sigma (q_{i+a} - q_i)(c^\dagger_{ci\sigma} c_{ci+a\sigma} + c^\dagger_{ci+a\sigma} c_{ci\sigma}) + \frac{K}{2}(q_{i+a} - q_i)^2 + \frac{1}{2M} p_i^2 \right], \tag{3}$$

where α_σ denotes the electron-phonon coupling strength. Thus, the starting Hamiltonian is

$$H = H_{\text{KLM+U}} + H_{\text{Holstein}} + H_{\text{SSH}}. \tag{4}$$

These phononic contributions may not describe the full complexity of the phononic couplings observed in real materials because of the phase-space constraint of any one-dimensional calculation. However, the results capture the essence of the Kondo lattice coexisting with phonons, and being an exact solution, it represents a vital source of information because of the lack of comparable solutions applicable to colossal magnetoresistance materials.

IV. THE EFFECTIVE HAMILTONIAN

A large class of one-dimensional many-electron systems may be described using bosonization techniques.[30] The electron fields may be represented in terms of collective density operators that satisfy bosonic commutation relations. Bosonic representations provide a nonperturbative description which, in general, are by far easier to evaluate than a formulation in terms of fermionic operators.

The underlying bosonization scheme follows standard procedures[30] by first decomposing the on-site operators into Dirac fields, $c_{x,\sigma} = \Sigma_\tau e^{ik_F x} \Psi_{\tau,\sigma}(x)$, where $k_F = \pi n/2$, with spinor components $\tau = \pm$ (+/− being the right/left movers) and $k_F = \pi n/2$. Next we bosonize the Dirac fields with $\Psi_{\tau,\sigma} = \exp(i\Phi_{\tau,\sigma})/\sqrt{2\pi\lambda}$, where $1/\lambda$ is the ultraviolet cutoff. For the scalar Bose fields, $\Phi_{\tau,\sigma}(x)$, and their conjugate momenta, $\Pi_{\tau,\sigma}(x)$, $\Phi_{\tau,\sigma}(x) = \int_{-\infty}^{x} dx' \Pi_{\tau,\sigma}(x')$, are used in standard Mandelstam representation by means of which a momentum cutoff via the Fourier transform is introduced $\Lambda(k) = \exp(-\lambda|k|/2)$. If the distance between the impurity spins is larger than λ, the electrons will behave as collective density fluctuations.[30] Thus, the Fermi fields can be represented in terms of density operators that satisfy Bose commutation relations

$$c_{\tau,x,\sigma} = \exp(i\tau k_F x) \exp i\{\theta_\rho(x) + \tau\phi_\rho(x) + \sigma[\theta_\sigma(x) + \tau\phi_\sigma(x)]\}/2, \tag{5}$$

where the Bose fields for $\nu = \rho, \sigma$ are defined by

$$\psi_\nu(x) = i(\pi/N) \sum_{k\neq 0} e^{ikx} [\nu_+(k) \pm \nu_-(k)] \Lambda(k)/k, \tag{6}$$

with + corresponding to the number fields $\psi_\nu = \phi_\nu$ and − to the current fields $\psi_\nu = \theta_\nu$. The charge (holon) and spin (spinon) number fluctuations are defined as $\rho_\tau(k) = \Sigma_\sigma \rho_{\tau,\sigma}(k)$, and $\sigma_\tau(k) = \Sigma_\sigma \sigma \rho_{\tau,\sigma}(k)$. All rapidly oscillating terms originating from, e.g., backscattering and umklapp processes are neglected, since they contribute only at exactly half filling. The localized d electrons can neither be bosonized nor Jordan-Wigner transformed since no direct interaction exists between them.

Substituting these representations into Eq. (1) gives the bosonized KLM Hamiltonian

$$H_{\text{KLM+U}} = \frac{1}{4\pi} \sum_{j,\nu} v_\nu \{\Pi_\nu^2(j) + [\partial_x \phi_\nu(j)]^2\} + \frac{J}{2\pi} \sum_j [\partial_x \phi_\sigma(j)] S^z_{\text{d},j} + \frac{J}{4\pi\lambda} \sum_j \{\cos[\phi_\sigma(j)] + \cos[2k_F j + \phi_\rho(j)]\} (e^{-i\theta_\sigma(j)} S^+_{\text{d},j} + \text{H.c.}) - \frac{J}{4\pi\lambda} \sum_j \sin[\phi_\sigma(j)] \sin[2k_F j + \phi_\rho(j)] S^z_{\text{d},j}. \tag{7}$$

The charge and spin velocities are given below.

Considering the phononic contributions, in standard bosonization language, Eq. (2) simplifies to $H^{\text{ph}} + H_1^{\text{el-ph}} + H_2^{\text{el-ph}}$, where

$$H^{\text{ph}} = \frac{1}{2N} \sum_p [\Pi_0^2(p) + \omega_0^2 \Phi_0^2(p)] + \frac{1}{2} \int dx [\Pi_\pi^2(x) + \omega_\pi^2 \Phi_\pi^2(x)], \tag{8}$$

and $\omega_0 = \omega_\pi = \sqrt{K/M}$ are their respective phonon frequencies. The electron-phonon forward-scattering term is simply

$$H_2^{\text{el-ph}} = \gamma_2 \frac{\sqrt{2}}{N} \sum_p [\rho_+(-p) + \rho_-(-p)] \Phi_0(p). \tag{9}$$

On the other hand, the rapidly oscillating phonon-assisted backscattering term will acquire an extra factor $\exp[\pm i\pi\delta n x] \equiv \exp[\pm i(2k_F - \pi)x]$, in the form

$$H_1^{\text{el-ph}} = \gamma_1 \sum_{\nu=\pm,\sigma} \int dx[\Psi^\dagger_{\nu,\sigma}\Psi_{-\nu,\sigma}e^{i\pi\nu\delta nx}]\Phi_\pi(x), \quad (10)$$

with $\gamma_1=\gamma_2=\beta/\sqrt{M}$, where we used the same subscripts for backscattering and forward scattering as in g-ology.[30]

In the continuum limit, the SSH term in contrast to the Holstein coupling, gives only two terms $H^{\text{ph}}+H_{-1}^{\text{el-ph}}$—the standard phononic component and a rapidly oscillating backscattering term. H^{ph} is given in Eq. (8), while the backscattering term $H_{-1}^{\text{el-ph}}$ differs from Eq. (10) only in a form factor

$$H_{-1}^{\text{el-ph}} = \gamma_{-1} \sum_{\nu=\pm,\sigma} \int dx[i\nu\Psi^\dagger_{\nu,\sigma}\Psi_{-\nu,\sigma}e^{i\pi\nu\delta nx}]\Phi_\pi(x), \quad (11)$$

with $\gamma_{-1}=4\alpha_\sigma/\sqrt{M}$. However, the fact that the forward-scattering term is missing means that the SSH coupling will not give any contribution to the effective Hamiltonian away from half filling.

Thus, the transformed Hamiltonian of Eq. (4) is

$$\begin{aligned} H = {} & \frac{1}{4\pi}\sum_{j,\nu} v_\nu\{\Pi_\nu^2(j) + [\partial_x\phi_\nu(j)]^2\} + \frac{1}{2N}\sum_p [\Pi_0^2(p) + \omega_0^2\Phi_0^2(p)] \\ & + \gamma_2\frac{\sqrt{2}}{N}\sum_p [\rho_+(-p) + \rho_-(-p)]\Phi_0(p) \\ & + \frac{1}{2}\int dx[\Pi_\pi^2(x) + \omega_\pi^2\Phi_\pi^2(x)] + \frac{J}{4\pi\lambda}\sum_j \{\cos[\phi_\sigma(j)] \\ & + \cos[2k_F j + \phi_\rho(j)]\}(e^{-i\theta_\sigma(j)}S^+_{\text{d},j} + \text{H.c.}) \\ & - \frac{J}{4\pi\lambda}\sum_j \sin[\phi_\sigma(j)]\sin[2k_F j + \phi_\rho(j)]S^z_{\text{d},j} \\ & + \frac{J}{2\pi}\sum_j [\partial_x\phi_\sigma(j)]S^z_{\text{d},j}. \end{aligned} \quad (12)$$

If holes are present in the array of d spins, all terms proportional to S are zero. The charge and spin velocities are

$$\begin{aligned} v_\rho &= v_F\sqrt{1 + U/\pi v_F - \beta^2/\pi K v_F}, \\ v_\sigma &= v_F\sqrt{1 - U/\pi v_F + \beta^2/\pi K v_F}, \end{aligned} \quad (13)$$

where the Fermi velocity is $v_F=2\sin(\pi n/2)$ in units of t.

It is important to note that a renormalization of the spinon-holon velocities appears here due to the Hubbard and phonon terms, which act oppositely on the corresponding velocities. Although the Hubbard term leads to a localization of the spinons and an increased hopping of the holons, thus supporting a magnetic ground state, the phonons delocalize the spins, but localize the charges and act destructively on the magnetic properties. It is worth mentioning that the Hubbard term alone already suffices to establish two time scales for the holon-spinon dynamics. But an important renormalization of the critical properties of the system is achieved through the variable phonon coupling, which, as will be shown below, establishes the existence of a Griffiths phase. The competition between the Hubbard and the phonon term obviously vanishes for $U=\beta^2/K$.

In the following, effects arising from the localized spin d impurities, double-exchange, the phonons, and Hubbard interactions will be discussed in more detail. The localized spin d impurities act via double exchange on the hopping electrons so as to preserve their spin when moving through the lattice in order to screen the localized spins that are in excess of the conduction electrons, i.e., $N \leqslant N_d > N_c$. This, in turn, leads to a tendency to align the localized spins and results in an additional screening energy for the conduction electrons.

V. LOCALIZED SPIN ORDERING

In order to determine rigorously the phase diagram and investigate the ordering of the local spins due to the formation of polarons, we first apply a unitary transformation. This is the simplest method for determining the ordering of the localized spins induced by the conduction electrons and it has been used successfully elsewhere.[22,23] This is achieved by choosing a basis of states for the unitary transformation in which competing effects become more transparent, i.e., a transformation that changes to a basis of states in which the conduction electron-spin degrees of freedom are directly coupled to the localized spins. Correspondingly, we choose the operator $\hat{S}=i(J/2\pi)\sqrt{v_F/v_\sigma^3}\Sigma_j\theta_\sigma(j)S^z_{\text{d},j}$, which is applied to Eq. (12) up to infinite order, thus avoiding truncation errors.

Second, we explicitly take into account the Luttinger liquid character of the Bose fields, i.e., use their noninteracting expectation values such that the effective Hamiltonian for the local spins is derived as

$$\begin{aligned} H_{\text{eff}} = {} & -\frac{J^2v_\sigma^2}{4\pi^2v_F}\sum_{j,j'}\int_0^\infty dk\cos[k(j-j')]\Lambda^2(k)S^z_{\text{d},j}S^z_{\text{d},j'} \\ & + \frac{J}{2\pi\lambda}\sum_j \{\cos[K(j)] + \cos[2k_F j]\}S^x_{\text{d},j} \\ & - \frac{J}{2\pi\lambda}\sum_j \sin[K(j)]\sin[2k_F j]S^z_{\text{d},j}. \end{aligned} \quad (14)$$

Here $K(j)$ arises from the unitary transformation and counts all the $S^z_{\text{d},j}$'s to the right of the site j and subtracts all those to the left of j: $K(j)=(J/2v_F)\Sigma_{l=1}^\infty(S^z_{\text{d},j+l}-S^z_{\text{d},j-l})$. This term gives the crucial difference between the Kondo lattice and dilute Kondo lattice, as will be explained in the following.

The most important term in Eq. (14) is the first one,

$$J_{\text{eff}}(j-j') = \frac{J^2v_\sigma^2}{4\pi^2v_F}\int_0^\infty dk\cos[k(j-j')]\Lambda^2(k). \quad (15)$$

This term, derived using an infinite-order unitary transformation, is exact, nonperturbative, and shows that a double-exchange ferromagnetic interaction appears for both $J>0$ and $J<0$ coupling and even in the dilute Kondo lattice model. This coupling is nonnegligible for $N_d>N_c$ and $j-j' \leqslant \lambda$ and its strength decreases with increasing distance between impurity spins. The value of J_{eff} is plotted for different values of U and β in Fig. 1.

Figure 1 shows clearly that the Hubbard interaction enhances double exchange and, consequently, J_{eff}. As noted

earlier, see the discussion following Eq. (13), this is because the Hubbard term leads to a localization of spinons and an increase in the hopping of holons, hence, increasing the double exchange. On the other hand, the electron-phonon interaction counteracts this effect by localizing the holons and thus decreasing J_{eff}.

Figure 1 also shows that the length λ characterizes the effective range of the double-exchange interaction. This interaction originates from the bosonization of the conduction electron band in the following way: at wavelengths larger than λ, the electrons combine to form collective density fluctuations, which involve large numbers of electrons satisfying bosonic commutation relations. This is the standard behavior of one-dimensional many-electron systems for weak interactions.[30] At wavelengths smaller than λ, the density fluctuations are not collective and lose the bosonic character. Since bosonization only applies to fluctuations beyond λ, the bosonization description is equivalent to keeping the electrons finitely delocalized within the range of λ, with the electrons preserving their spin over this range. Equation (15) describes the ordering induced on the localized spins by the finitely delocalized electrons. Thus, λ corresponds to the effective delocalization length related to the spatial extent of the polarons (polaron radius), i.e., the effective range of double-exchange, as shown in Fig. 2. Here the case $J>0$ is shown, where the (z component) spin of the electron is always opposite to that of the impurity spin within the magnetic polaron, due to the tendency for Kondo singlet formation. This state corresponds to the $E_{0,J>0}$ and $|\psi_0\rangle_{J>0}$ solution of the two-site problem presented in Sec. II. Thus, Kondo singlet formation has been taken into account indirectly, via the effective range of the double-exchange interaction. In the single impurity ($N_d=1$) and/or half filled ($N_c=N_d$) limits our result reduces to the well-known Kondo singlet physics of the single impurity Kondo model, as will be discussed in detail in Sec. VI.

For the $J<0$ case, the magnetic polarons are the same as shown in Fig. 2, with the exception that the spin of the electron is always parallel to the impurity spin. Spin triplet formation dominates the $J<0$ case, corresponding to the $E_{0,J<0}$ and $|\psi_0\rangle_{J<0}$ solution of the two-site problem in Sec. II.

Double-exchange becomes inefficient if the distance between the impurity spins is larger than λ. In general λ has a complex behavior, depending on J, U, β, and N_c. For large distances and low density, Eq. (15) gives an effective range for the double-exchange, which decays exponentially with a characteristics scale $\sqrt{2/|J|}$. Hence, in the following we will use for λ its low density (e.g., in the example depicted in Fig. 2) value: $\lambda \approx \sqrt{2/|J|}$. And since the interaction Eq. (15) is short range for all finite λ we approximate it by its nearest-neighbor form

$$J_{\text{eff}} = \frac{J^2 v_\sigma^2}{2\pi^2 v_F} \int_0^\infty dk \cos k \Lambda^2(k). \tag{16}$$

Here we emphasize again that Eq. (16) is valid for both $J>0$ and $J<0$ couplings. Since the $J>0$ case is usually not considered in discussions of the KLM, we emphasize the following points: (i) the term originates, via bosonization and

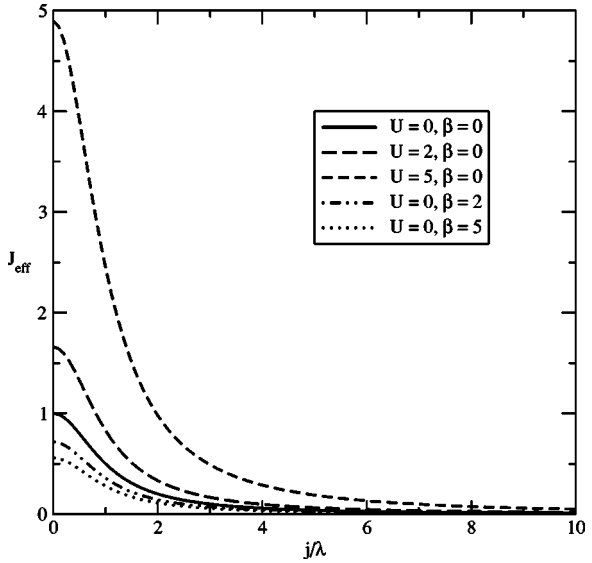

FIG. 1. The range of the ferromagnetic interaction Eq. (15) for different values of U and β. J_{eff} is the interaction strength in units of $J^2 v_\sigma^2 / 4\pi^2 v_F$.

then the unitary transformation, from the kinetic energy term $-t\Sigma_{j,\sigma}(c_{j,\sigma}^\dagger c_{j+1,\sigma} + \text{H.c.})$ and the forward scattering part of $(J/2)\Sigma_j (n_{j\uparrow} - n_{j\downarrow}) S_j^z$ $(n_{j\sigma} = c_{j\sigma}^\dagger c_{j\sigma})$ in the KLM Hamiltonian equation (1). (Note that the Bose representations for the electrons in these terms are exact.) (ii) Equation (16) is independent of the sign of J and takes the same form for any magnitude S_j^2 of the localized spins. (iii) Since Eq. (16) is of order J^2, whereas the remaining terms in the transformed Hamiltonian Eq. (14) are of order J, the interaction Eq. (16) dominates the ordering of the localized spins as J increases. All these properties are identical to those of a double-exchange interaction. This leads us to identify Eq. (16) as the double-exchange interaction in the KLM. We also emphasize that Eq. (16) is ferromagnetic for all (possible) choices of the cutoff function $\Lambda(k)$.

Based on property (i) above, a simple characterization can be given for the double-exchange valid at low-conduction band filling. The simple Hamiltonian term (1) satisfies a standard nonlinear Schrödinger equation: $\partial_x^2 \psi_\sigma(x) + (J m_{\text{el.}}/2)|\psi_\sigma(x)|^2 \psi_\sigma(x) = 2 m_{\text{el.}} E \psi_\sigma(x)$ [$m_{\text{el.}}$ being the bare electron mass, and $\psi_\sigma(x)$ the electronic wave function] with soliton solutions $\psi_\sigma(x) \propto e^{ix}\,\text{sech}(x\sqrt{J m_{\text{el.}}/4})$ (see Ref. 31).

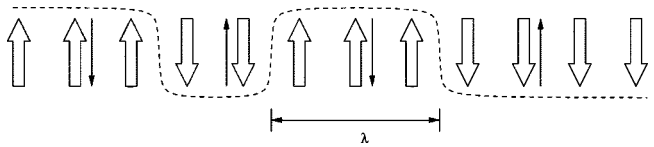

FIG. 2. A snapshot of the magnetic polarons for the case $J>0$. ⇑ (⇓) and ↑ (↓) refers to the z component of the impurity and conduction electrons spins. The dashed curve represents the spin domain walls (kink-antikink pairs). The electrons will oscillate between these domains walls and hence couple the impurity spins through double-exchange (for details see text). λ is the average length of the polarons, i.e., the effective range of the double-exchange.

These soliton solutions correspond to spin domain walls of finite size (kink-antikink pairs) and lead to a gain in electronic energy of $-\sigma$ for antiferromagnetic coupling, and of $+\sigma$ for the ferromagnetic case, as shown in Fig. 2. Physically the solutions resemble the dressing of the electron by a finite range of parallel (antiparallel) local spins and, consequently, can be identified with polaronic-type objects. From the previous considerations it can also be concluded that, when including the interactions with the phonons, the tendency toward charge localization is enhanced and increases this polaronic effect. Since the lattice also experiences a renormalization because of the coupling to the electronic degrees of freedom, substantial ionic displacement patterns will develop and the formation of magnetoelastic polarons takes place. Similar results are obtained by decoupling electronic and phononic degrees of freedom through a homogeneous Lang-Firsov transformation, where the localization stems from band narrowing. In accordance with previous results, the polaron radius is characterized by a length scale proportional to $\sqrt{2/|J|}$.

This length scale differs from the free conduction electrons mean free path and gives rise to competing time scales: slow motion of the polaronic carriers and fast motion of the free electrons, thus providing dynamics of two types of particles and a close analogy to a two-fluid scenario.[32,33] Since the polarons are, in general, randomly distributed within the local spin array, these states can be viewed as intrinsic inhomogeneities involving spin fluctuations and short-range spin correlations. Hence, these slow dynamics will exhibit a peak in the spin-structure factor at $2k_F-\pi$ instead of the simple $2k_F$ RKKY signal. This $2k_F-\pi$ peak of in the spin-structure factor has been observed in all numerical approaches for both $J>0$[18–21] and $J<0$.[34] As mentioned previously, the difference between the $J>0$ and $J<0$ polarons appears in the local ordering of the conduction electron spin with the impurity spins: for $J>0$ the conduction electron spin will be always aligned antiparallel to the localized spins due to the tendency to form Kondo singlets, while for $J<0$ the two spins will be aligned parallel due to the dominating triplet states. The presence of of on-site Kondo singles and the effect of Kondo screening will be analyzed in detail in Sec. VI.

Beyond the numerical support, the available rigorous results support this polaronic picture: for vanishingly small fillings the exact ground-state wave function, obtained using the Perron-Frobenius theorem,[35] is a large magnetic polaron of width $\sqrt{2/|J|}$ with aligned localized spins and the conduction electron spin being antiparallel ($J>0$) or parallel ($J<0$) to the localized spins (for more details also see Refs. 24 and 36).

VI. THE PHASE DIAGRAM

In the following discussions, we mainly concentrate on antiferromagnetic ($J>0$) coupling, as this case has not been as extensively studied as the ferromagnetic one. However, differences that appear in the $J<0$ solution will be noted.

For the Kondo lattice model, $K(j)\approx 0$ as the number of localized spins to the left and right of a given site j are the same. If, however, we have a small concentration of holes in the array of localized spins, then—opposite to the previous case—$K(j)$ is nonvanishing since the hole spins are no longer necessarily equally distributed to the left and the right of a given site. This yields $K(j)\approx(-1)^j(J/2v_F)$, which gives rise to a staggered field and antiferromagnetic ordering.[33] This distinguishes the dilute case from the standard Kondo lattice model, where only three phases appear:[36] the ferromagnetic, paramagnetic, and Kondo spin-liquid phases. Among these phases, the Kondo spin-liquid phase only appears at half filling and represents an effective model for Kondo insulators.[36–38] This phase is dominated by Kondo singlet physics and exhibits finite-temperature behavior similar to the single-impurity Kondo model.[36]

The remaining two phases are typical for the dilute limit, and since our major interest here is ferromagnetism and to explore the occurrence of ferromagnetism in the presence of the Hubbard and phonon terms, we will address only this limit. The properties of the Kondo spin-liquid phase will only be briefly presented later on this section. Hence, focusing on the ferromagnetic phase, where $K(j)$ is vanishingly small, the transition between the paramagnetic and the ferromagnetic state will be controlled by the first two terms of Eq. (14).

Accordingly, H_{eff} reduces to a quantum transverse-field Ising chain. This model without backscattering is known[39] to undergo a quantum phase transition from a ferromagnetic to a paramagnetic phase. In the case of Eq. (14), where a backscattering is also present, a similar phase transition occurs as the coupling J is decreased: the conduction electrons become less strongly bound to the localized spins and tend to extend over spatial ranges beyond the effective range λ of double-exchange ordering. Double exchange becomes less effective, i.e., the magnetic polarons are loosely bound and regions of ordered localized spins begin to interfere as the conduction electrons become extended. The interference leads to spin-flip processes given by the transverse field in H_{eff}.

The transverse field, $h(j)=(J/2\pi\lambda)[1+\cos(2k_Fj)]$, in H_{eff}, includes two low-energy spin-flip processes by means of which the conduction electrons disorder the localized spins. One spin-flip process is backscattering, which is accompanied by a momentum transfer of $2k_F$ from the conduction electrons to the localized spins. Since the chain of localized spins will tend to order so as to reflect this transfer, the transverse-field corresponding to backscattering spin-flips is sinusoidally modulated by $2k_F$. The other low-energy spin-flip process in H_{eff} is forward scattering. This involves zero momentum transfer to the localized spins, and the corresponding transverse field is a constant (i.e., has modulation zero).

However, away from half filling, the transverse field $h(j)$ will have an incommensurate modulation $2k_F$ with respect to the underlying lattice of localized spins. Hence, the conduction band is unable to either totally order or totally disorder the lattice as the ferromagnetic-to-paramagnetic transition occurs. There remain dilute regions of double-exchange-ordered localized spins or magnetic polarons in the paramagnetic phase as only a quasicommensurate fraction of the conduction electrons become weakly bound and become free to scatter along the chain. The remaining ordered regions are

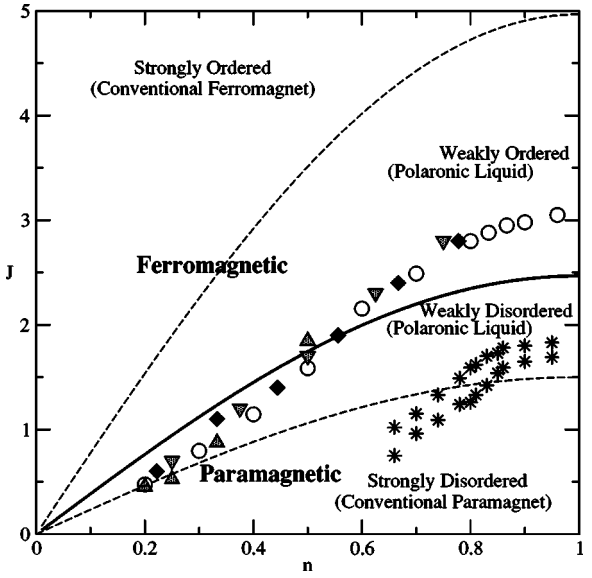

FIG. 3. The ground-state phase diagram of the standard KLM, where n is the conduction electron band filling. The solid (critical) line is from Eq. (18). The dashed lines separate strongly ordered (conventional ferromagnet) and/or disordered (conventional paramagnet) phases from their weak Griffiths phase (polaronic liquid) counterparts. The numerically determined FM-PM transition points are the followings: down triangle and diamond are exact numerical diagonalization results from Ref. 19 for eight- and nine-chain, respectively. Up triangle and circle are DMRG results for 60 sites (Ref. 20) and 200 sites (Ref. 21), respectively. The stars represent the numerically determined (DMRG results from Refs. 18 and 21) crossover region into the polaronic liquid state.

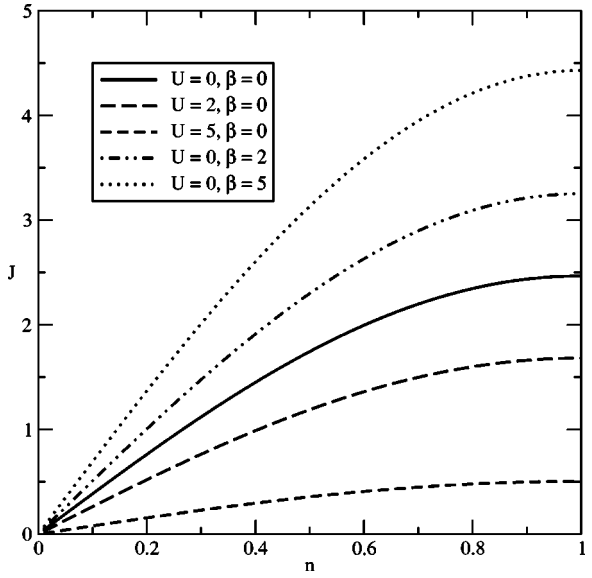

FIG. 4. The quantum critical line [Eq. (18)] describing the ferromagnetic transition for different values of U and β, where n is the conduction electron band filling. For each of these examples the ferromagnetic phase is above the phase-transition curve.

sufficiently dilute to prevent long-range correlations, but their existence dominates the low-energy properties of the localized spins near the transition.

These considerations motivated us to treat the transverse field as a random variable. The effective Hamiltonian is thus equivalent to a random transverse-field Ising model:[22]

$$H_{\mathrm{crit}} = -J_{\mathrm{eff}} \sum_j S^z_{\mathrm{d},j} S^z_{\mathrm{d},j+1} - \sum_j h_j S^x_{\mathrm{d},j}, \tag{17}$$

where J_{eff} is given in Eq. (16) and since the interaction Eq. (15) is short range for all finite λ, gives in Eq. (17) a nearest-neighbor Ising term. The random fields h_j are generated by $(1+\cos[2k_F j])$ at large distances, where $\cos[2k_F j]$ oscillates unsystematically with respect to the lattice. The large values $\cos[2k_F j] \approx 1$, which are responsible for spin flips, are then well separated and driven by a cosine distribution analogous to spin-glasses.[40]

Using the extensive real-space renormalization-group results of this model by Fisher,[42] we determine the location of the quantum critical line describing the paramagnetic-to-ferromagnetic transition at

$$J_{\mathrm{crit}} = (\pi^2/4)\sin(\pi n/2)\{1 - U/[2\pi \sin(\pi n/2)] + \beta^2/[2\pi K \sin(\pi n/2)]\}^{1/2}. \tag{18}$$

For values $J < J_{\mathrm{crit}}$ a paramagnetic state exists that is dominated by polaronic fluctuations. For $J > J_{\mathrm{crit}}$ ferromagnetism appears. The transition between these phases is of order-disorder type with variable critical exponent $\delta = \ln(J_{\mathrm{crit}}/J)$.

The behavior described by H_{crit} is simply understood in terms of magnetic polarons introduced previously (see also Fig. 2). Considering for the moment the standard KLM model, a summary of the known results[22] is presented in Fig. 3. Reducing J from intermediate values in the ferromagnetic phase, the infinite cluster characterizing strong ferromagnetism is broken up into several large clusters as the quantum fluctuations h_j, controlled by the spin-flip interactions, become stronger. The individual clusters are the spin polarons depicted in Fig. 2. These magnetic polarons are weakly ordered in this phase, i.e., form a polaronic liquid that exists for $-0.7 < \delta < 0$ hence with the upper boundary determined by $J \approx 2J_{\mathrm{crit}}$ (see Fig. 3). This is not a true transition line, but rather marks the crossover to a Griffiths phase[41] characterized by singularities in the free energy over the whole range of δ. For small δ the correlation length is $\xi \sim \delta^{-2}$, beyond which the system is ordered. The spontaneous magnetization $M_0 \propto |\delta|^{\gamma}$, with $\gamma = (3-\sqrt{5})/2 \approx 0.38$,[42] while for small applied fields H the magnetization $M(H) \propto M_0[1 + \mathcal{O}(H^{2|\delta|}\delta \ln H)]$; the susceptibility is infinite with a continuously variable exponent. The mean correlation function is given by $(\xi/x)^{5/6} e^{-x/\xi} \exp[-3(\pi x/\xi)^{1/3}]$ for $x \gg \xi$.[42]

Further lowering J, we reach the true phase transition [Eq. (18)]. The correlation length is infinite, the magnetization $M(H) \propto |\ln H|^{-\gamma}$ for small H, and the mean correlation function is critical $x^{-\gamma}$. The transition curve for different values of U and β is shown in Fig. 4. As argued previously, the Hubbard interaction makes the ferromagnetic phase more robust, as it increases the strength of the double exchange and, as such, the length of the magnetic polarons.

Calculating the effective length of polarons, λ on the transition line (see Fig. 5) supports this finding. The length of the polarons increases strongly with U, hence making the ferro-

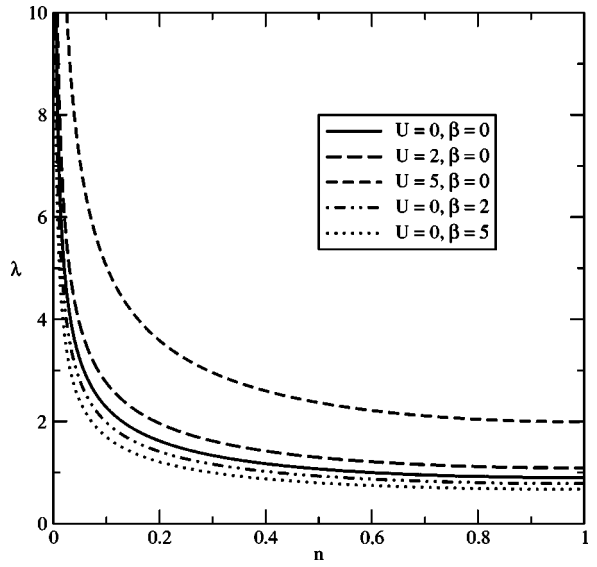

FIG. 5. The effective range λ of the double-exchange interaction in units of the lattice spacing against the conduction electron band filling n on the critical line.

magnetic phase more difficult to break up. However, the consequence of this effect is that the Griffiths phase below the transition will diminish strongly or vanish in most cases.

The effect of phonons is opposite to this. The phonons act destructively on the magnetic properties. The ferromagnetic phase becomes smaller (see Fig. 4) and the length of the polarons are slightly decreased in the presence of the phonons as shown in Fig. 5. But, as will be explained later, the boundaries of the lower Griffiths phase will remain the same. Thus, contrary the the effect of U, where the Griffiths phase vanishes, for strong phononic couplings the magnetoelastic polarons extend over a much larger phase space and will dominate the phase diagram of the KLM.

It is interesting to note that as we approach half filling, i.e., $n \rightarrow 1$, λ becomes equal to the lattice spacing. This means that the magnetic polaron reduces to a Kondo singlet, as it should be, since the half-filling limit of the Kondo lattice model is a Kondo spin-liquid phase[36–38] dominated by Kondo singlet physics.[36] A spin-liquid phase is obtained for the $J<0$ case also. However in this case Kondo triplet states are formed. This is a very general requirement, true for Kondo lattice models in any dimensions.

A rigorous theorem holds for the half-filled Kondo lattice in any dimension on a bipartite lattice:[36,43,44] for $J>0$ the ground state is unique and has zero total spin. The same conclusion holds for $J<0$ provided the two sublattices have the same number of sites. Beyond the rigorous proof that the ground state is a total spin singlet in any dimension, there is substantial evidence that the ground state also has a spin gap at least in one dimension. The ground state of the half-filled Kondo lattice thus forms a spin liquid for any sign of J.

For large $J>0$ the ground state at half filling consists of N on-site Kondo singlets. There is a spin gap of size J to an on-site triplet state, and a larger charge gap of $3J/2$, corresponding to the hopping of a conduction electron to a neighboring site. The persistence of the spin gap (and a larger charge gap) down to arbitrarily small coupling strengths $J>0$ has been established by numerical simulations [36,45] and by approximate analytical methods.[38,46] Spin gaps are also observed in bosonization treatments of the one-dimensional half-filled Kondo lattice (see Ref. 47 for $J>0$ and Ref. 48 for $J<0$). Nonetheless, the nature of the gap for $J<0$ is different. For $J>0$, the strong-coupling behavior is that of the Kondo spin liquid, while for $J<0$ it scales to a spin 1 chain and reduces to a Haldane gap state at strong-coupling.[45]

As noted in Sec. II, the singlet ground state and spin gap in the half-filled Kondo lattice permits a formal identification of this phase with the single-impurity Kondo model, with the Kondo temperature the energy of the spin gap. Also, the correlation functions have a smooth crossover, as the correlations between nearest-neighbor localized spins in the half-filled Kondo lattice model are antiferromagnetic for any sign of the coupling. This may be understood beginning from the $|J|=\infty$ limits, where there is one conduction electron localized at each site. At strong but finite coupling there is weak virtual conduction-electron hopping to neighboring sites. By the Pauli principle, this is possible only if the conduction electron on the neighboring site has opposite spin. For strong but finite ferromagnetic or antiferromagnetic coupling, the weak antiferromagnetism of the localized conduction electrons induces a similar antiferromagnetic ordering on the underlying localized spins. Strong antiferromagnetism at weak coupling is expected on the basis of the RKKY interaction, which oscillates in sign with wave vector $2k_F$. At half filling, $k_F=\pi/2a$, and so the RKKY interaction changes sign at neighboring lattice sites. These expectations are supported by the results of numerical simulations for $J>0$,[18,37] and by perturbation theory at large ferromagnetic couplings.[45]

The other obvious limit where on-site Kondo singlets appear is $J=\infty$. Contrary to the half-filled case discussed above, where the Kondo singlets are localized, in this case the nearest-neighbor transfer of the conduction electrons allows these on-site Kondo singlet pairs to move. In fact it was shown by Lacroix[49] that the $J=\infty$ Kondo lattice can be mapped rigorously to a $U=\infty$ Hubbard model. An empty site of the Hubbard model corresponds to a Kondo singlet and a site occupied by a spin corresponds to an empty site (thus an unpaired localized spin) of the Kondo lattice. Because of the lack of double occupancy and only nearest-neighbor hopping, the electrons in the $U=\infty$ Hubbard model can never move past one another; given an ordering of electrons, say from left to right, that ordering is preserved by the action of the Hamiltonian. In addition there are no spin-flip interactions; therefore, the spin degrees of freedom are completely degenerate. This degeneracy does not persist away from the $J=\infty$ case, and it was shown in Ref. 50 (see also Ref. 36) using a perturbative expansion with respect to t/J, that the spin degeneracy is lifted and the ground state is completely polarized. This leads to the peculiar situation where for any band filling the one-dimensional KLM is always ferromagnetic in the presence of on-site Kondo singlets. This ferromagnetism is identical[50] to the Nagaoka phase from the $U=\infty$ Hubbard model.

A detailed analysis is also presented in Ref. 36 whether the KLM undergoes a qualitative change at large J from the polaronic picture of Ref. 35 to the $J=\infty$ Nagaoka-type

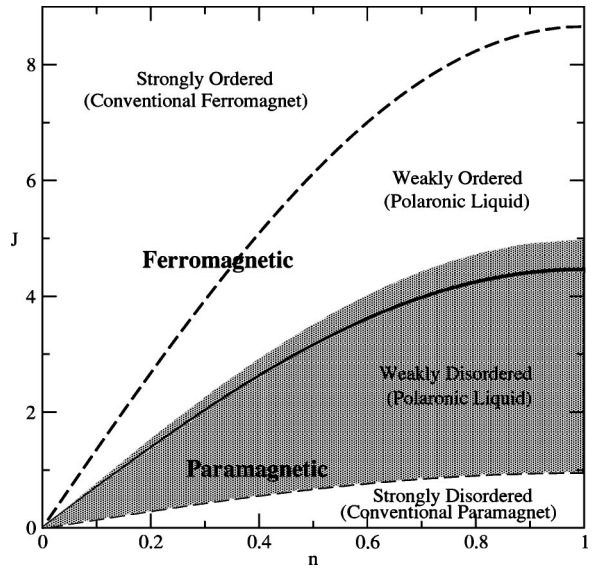

FIG. 6. The ground-state phase diagram for $U=0$ and $\beta=5$. The solid line is true phase-transition line from Eq. (18). The dashed lines separate the conventional ferromagnet and/or paramagnet phases from their weakly disordered (polaronic liquid) counterparts. Note the extent of the polaronic liquid phases compared to the $U=0$ and $\beta=0$ standard KLM (shaded region) corresponding to Fig. 3.

mechanism. It was concluded[36] that that the mechanism supporting Nagaoka is always weaker for any finite J than that of the polaronic mechanism and, hence, a Nagaoka-type ferromagnetic phase only appears at strictly $J=\infty$. Clearly this ferromagnetic phase in the strong-coupling regime is a special feature of the one-dimensional KLM. It is well known[36] that a clear difference exists between the one- and higher-dimensional systems, in the latter the spin degeneracy is lifted for any band filling away from half filling.

In the $J>0$ KLM model, away from half filling and the strong-coupling limits, a strong tendency toward Kondo singlet formation is always present. In fact, the two-site problem analyzed in Sec. II shows that there is always a competition between double-exchange ordering and Kondo singlet formation. This is also true for the bosonized solution of KLM given in Eq. (7) or $H_{\rm crit}$ from Eq. (17): Kondo screening of the local moments will be always present for any $J>0$ away from half filling. This has been extensively studied previously (see Ref. 23). In order to make Kondo screening more transparent we rewrite Eq. (7) to explicitly show the different components of the scattering matix

$$
\begin{aligned}
H_{\rm KLM+U} = & \frac{1}{4\pi}\sum_{j,\nu} v_\nu\{\Pi_\nu^2(j) + [\partial_x\phi_\nu(j)]^2\} \\
& + \frac{J_\parallel^f}{2\pi}\sum_j [\partial_x\phi_\sigma(j)]S^z_{{\rm d},j} + \frac{1}{4\pi\lambda}\sum_j \{J_\perp^f \cos[\phi_\sigma(j)] \\
& + J_\perp^b \cos[2k_F j + \phi_\rho(j)]\}(e^{-i\theta_\sigma(j)}S^+_{{\rm d},j} + {\rm H.c.}) \\
& - \frac{J_\parallel^b}{4\pi\lambda}\sum_j \sin[\phi_\sigma(j)]\sin[2k_F j + \phi_\rho(j)]S^z_{{\rm d},j}, \quad (19)
\end{aligned}
$$

where f and b denote forward-scattering and backscattering terms, respectively; and in our case, $J_\parallel^f = J_\parallel^b = J_\perp^f = J_\perp^b \equiv J$. This way of writing the Kondo coupling is borrowed from the single-impurity model,[51] where it has been shown that the Kondo screening effect originates from $J_\perp^f$ and the associated Kondo scale has a power-law dependence on $J_\perp$. This is also true for the Kondo lattice, and, in particular, for the one-dimensional model[23] the energy associated with the Kondo screening is $\propto J_\perp$ and the Kondo resonance energy is $\propto J_\perp^2$. The competition between double-exchange and Kondo screening is also evident in the effective Hamiltonian equation (17), where the double-exchange originates from $J_\parallel^f$, while Kondo screening is taken into account in $h_j \propto J_\perp^f$.

Returning to the analysis of the obtained phase diagram (Fig. 4), immediately below the critical line ($\delta>0$), the system represents a weakly disordered Griffiths phase. The remaining polarons occupy a small fraction of the system length but behave as if they are still in the ordered phase; their magnetization δ^β per unit length is identical to M_0 of the weakly ordered phase.[42] These remaining rare polarons dominate the low-energy physics. Hence, crossing the phase transition line disorders the polarons. The transition is, indeed, an order-disorder transition of the magnetic polarons. This regime can be viewed as a paramagnet with locally ordered ferromagnetic regions. This scenario resembles a two-fluid picture, i.e., a polaronic liquid, with intrinsic inhomogeneities, which involves spin fluctuations and short-range spin correlations.

In this weakly disordered phase, the magnetization $M(H) \propto \delta^\gamma\{H^{2\delta}[\delta\ln(1/H)+{\rm const.}]+\mathcal{O}[H^{4\delta}\delta\ln(1/H)]\}$; thus $M(H)$ has a power-law singularity with a continuously variable exponent 2γ; as in the weakly ordered phase the susceptibility is infinite.

The mean correlation function decays less rapidly than in the weakly ordered phase, but takes the same form $(\xi/x)^{5/6}e^{-x/\xi}\exp[-3/2(\pi x/\xi)^{1/3}]$ for $x \gg \xi = 1/\delta^2$. According to $H_{\rm crit}$, the weakly disordered Griffiths phase extends down to $J=0$. However, as the disorder increases, the third term in $H_{\rm eff}$ is no longer negligible. At very low J, the last two terms in $H_{\rm eff}$ will dominate; this corresponds to free spins in a field with dominant correlations at $2k_F$ of the conduction band, and is responsible for the observed peak in the localized spin-structure factor.[18–21] This is the strongly disordered conventional paramagnetic phase (see Fig. 3).

As the boundary of this Griffiths phase is governed by the full $H_{\rm eff}$ from Eq. (14) rather than $J_{\rm crit}$ only, it will not be effected by U and β. This explains why the extent of this Griffiths phase increases dramatically in the presence of phonons and vanishes for large U. Thus the phonons indeed will enhance charge localization, increase the polaronic effect, and act destructively on the spin ordering. In the presence of phonons, these magnetoelastic polarons will dominate a larger phase space below and above the ferromagnetic transition compared to the standard KLM. This is shown explicitly in Fig. 6, where the $\beta=5$ case is compared to the $\beta=0$, and $U=0$ in both cases. It can be seen that the polaronic liquid occupies a much larger phase space in the first case compared to the standard KLM (shaded region). This proves that, at least in the one-dimensional KLM the local inhomogeneities are enhanced by phonons, creating magne-

toelastic polarons similar to intrinsic mesoscopic patterns from two-fluid model phenomenologies.

It is interesting to mention that similar behavior is expected in higher dimensions also. As shown in Ref. 54, the randomness generated through local inhomogeneities is the driving force, rather then dimensionality, in any real-space renormalization approach. Thus most of the properties presented previously will survive in higher dimensions. This have been confirmed also by extensive numerical calculations.[52]

An important prediction of our theory is the finite temperature behavior of the polaronic liquid phase below the transition line, the so-called weakly disordered paramagnetic phase. This is the region of the phase diagram, which is enhanced by phonons and as such dominated by magnetoelastic polarons, as explained previously. Here, following closely Ref. 42, we can determine the finite temperature susceptibility. At small temperatures the weakly coupled polarons behave as free spins with momenta $\delta^{\gamma-1}\ln(T^*/T)$ and the susceptibility will become $\chi_{\text{polaron}} \approx \delta^{2\gamma}(T/T^*)^{2\delta-1}\ln^2(T/T^*)$. T^* is a temperature scale at which the renormalization flow is stopped when the temperature fluctuation scale equals the quantum fluctuation.

The susceptibility diverges at $T \to 0$ in the Griffiths phase as expected,[41] However, if δ increases, e.g., $\delta \approx 1/2$ the system moves away from criticality, the susceptibility at zero temperature will be finite and will no longer be dominated by the large rare polarons but rather by the more typical smaller ones, becoming a strongly disordered phase. On the temperature scale, this corresponds to increasing the temperature. Thus, at higher temperatures the susceptibility will become $\chi_{\text{polaron}} \approx (T/T^*-1)\ln(T/T^*) = (1-T/T^*)\ln(T^*/T)$. Interestingly, this is identical to the phenomenological form of the susceptibility that has been associated with heavy quasiparticles in all heavy fermion compounds.[32] For these compounds T^* is the temperature at which the heavy quasiparticle liquid starts to emerge from a standard Kondo lattice behavior. Note that in our approach of deriving χ_{polaron} we moved away from the critical point, in agreement with recent calculations[53] that the heavy fermion systems are in the vicinity off, but not on a Griffiths singularity.

VII. CONCLUSIONS

In summary, we have derived an effective Hamiltonian from a one-dimensional Kondo lattice model extended to include effects stemming from coupling to the lattice and in the presence of an on-site Hubbard term, which accounts for the conduction electron Coulomb repulsion. The results are (i) a ferromagnetic phase appears at intermediate $|J|$ because of forward scattering by delocalized conduction electrons. (ii) Ferromagnetism is favored by the Hubbard term, while it is suppressed by the electron-phonon coupling. (iii) The paramagnetic phase is characterized by the coexistence of polaronic regimes with intrinsic ferromagnetic order and ordinary conduction electrons. (iv) In the paramagnetic phase, two time scales compete with each other—reminiscent of a two-fluid model—and the variability of the critical exponents suggests the existence of a Griffiths phase.

The results are related to the small-doping regime of CMR materials, which are ferromagnets at low temperatures, since here the coupling to the phonons has been shown to dominate the paramagnetic-ferromagnetic phase transition. Note that moving away from this criticality into the weakly disordered polaronic liquid phase the results, in particular, the finite temperature susceptibility, show behavior characteristic to all heavy fermion compounds.[32]

In regard to the CMR materials, it is interesting to point out the discrepancy between infinite-dimensional calculations and the present one-dimensional results. Many approximate calculations to model CMR[14] have been made in dynamical mean-field theory, which is an infinite-dimensional approximation and therefore incapable of capturing spatial inhomogeneities. In the present work we have approached the CMR materials via a one-dimensional approximation, but with techniques able to describe fluctuations of short-range order. Our results show that strong intrinsic spatial inhomogeneities of Griffiths type dominate the behavior of the Kondo lattice. Consequently, the inhomogeneities exhibit clear statistical scaling properties as a function of the proximity to a quantum (order-disorder) critical point. The phonons enhance the inhomogeneities, which, in a good approximation behave as a supercritical (metastable) phase of a two-fluid model.

Even though various bosonization schemes have been used for the one-dimensional KLM,[22,23] non of the previous approaches took into account phonons. The inclusion of phonon degrees of freedom has been shown here to be relevant in creating local magnetic inhomogeneities. It is important to emphasize that the properties of the system are controlled by intrinsic inhomogeneities. This means that, in a renormalization-group approach, the dimensionality should not matter.[52,54] Thus, a similar behavior is expected in realistic two and three dimensions, which clearly merit further detailed study.

ACKNOWLEDGMENTS

One of the authors (A.R.B.) acknowledges stimulating discussion with N. J. Curro concerning the data in Ref. 32. Work at Los Alamos is supported by the US DOE.

[1] C. W. Searle and S. T. Wang, Can. J. Phys. **48**, 2023 (1970); K. Kubo and N. Ohata, J. Phys. Soc. Jpn. **63**, 3214 (1972).

[2] S. M. Hayden, G. H. Lander, J. Zarestky, P. J. Brown, C. Stassis, P. Metcalf, and J. M. Honig, Phys. Rev. Lett. **68**, 1061 (1992).

[3] C. H. Chen, S-W. Cheong, and A. S. Cooper, Phys. Rev. Lett. **71**, 2461 (1993).

[4] H. Kawano, R. Kajimoto, H. Yoshizawa, Y. Tomioka, H. Kuwahara, and Y. Tokura, Phys. Rev. Lett. **78**, 4253 (1997).

[5] Y. Tomioka, A. Asamitsu, H. Kuwahara, Y. Moritomo, and Y. Tokura, Phys. Rev. B **53**, R1689 (1996).

[6] J. Q. Li, Y. Matsui, T. Kimura, and Y. Tokura, Phys. Rev. B **57**, R3205 (1998).

[7] Y. Moritomo, A. Nakamura, S. Mori, N. Yamamoto, K. Ohoyama, and M. Ohashi, Phys. Rev. B **56**, 14879 (1997).
[8] C. H. Chen and S-W. Cheong, Phys. Rev. Lett. **76**, 4042 (1996).
[9] E. O. Wollan and W. C. Koehler, Phys. Rev. **100**, 545 (1955).
[10] H. L. Liu, S. L. Cooper, and S.-W. Cheong, Phys. Rev. Lett. **81**, 4684 (1998); W. Bao, J. D. Axe, C. H. Chen, and S-W. Cheong, *ibid.* **78**, 543 (1997).
[11] S. Mori, C. H. Chen, and S-W. Cheong, Nature (London) **392**, 473 (1998).
[12] M. Uehara, S. Mori, C. H. Cheng, and S-W. Cheong, Nature (London) **399**, 560 (1999).
[13] C. Zener, Phys. Rev. **82**, 403 (1951).
[14] See, for example A. J. Millis, P. B. Littlewood, and B. I. Shraiman, Phys. Rev. Lett. **74**, 5144 (1995); H. Röder, J. Zang, and A. R. Bishop, *ibid.* **76**, 1356 (1996); and the references cited therein.
[15] E. Dagotto, S. Yunoki, A. L. Malvezzi, A. Moreo, J. Hu, S. Capponi, D. Poilblanc, and N. Furukawa, Phys. Rev. B **58**, 6414 (1998); S. Yunoki, J. Hu, A. L. Malvezzi, A. Moreo, N. Furukawa, and E. Dagotto, Phys. Rev. Lett. **80**, 845 (1998); H. Yi, N. H. Hur, and J. Yu, Phys. Rev. B **61**, 9501 (2000); Y. Motome and N. Furukawa, J. Phys. Soc. Jpn. **69**, 3785 (2000); W. Koller, A. Prüll, H. G. Evertz, and W. von der Linden, Phys. Rev. B **67**, 174418 (2003).
[16] See, for example, P. A. Lee, T. M. Rice, J. W. Serese, L. J. Sham, and J. W. Wilkins, Comments Condens. Matter Phys. **12**, 99 (1986).
[17] P. W. Anderson and H. Hasegawa, Phys. Rev. **100**, 675 (1955); P.-G. de Gennes, Phys. Rev. **118**, 141 (1960).
[18] M. Troyer and D. Würtz, Phys. Rev. B **47**, 2886 (1993); S. Moukouri and L. G. Caron, *ibid.* **52**, R15723 (1995); N. Shibata and K. Ueda, J. Phys.: Condens. Matter **11**, R1 (1999); I. P. McCulloch, A. Jouzapavicius, A. Rosengren, and M. Gulacsi, Philos. Mag. Lett. **81**, 869 (2001); A. Jouzapavicius, I. P. McCulloch, M. Gulacsi, and A. Rosengren, Philos. Mag. B **82**, 1211 (2002).
[19] H. Tsunetsugu, M. Sigrist, and K. Ueda, Phys. Rev. B **47**, 8345 (1993).
[20] S. Caprara and A. Rosengren, Europhys. Lett. **39**, 55 (1995).
[21] I. P. McCulloch, A. Juozapavicius, A. Rosengren, and M. Gulacsi, Phys. Rev. B **65**, 052410 (2002).
[22] G. Honner and M. Gulacsi, Phys. Rev. Lett. **78**, 2180 (1997); Phys. Rev. B **58**, 2662 (1998).
[23] O. Zachar, S. A. Kivelson, and V. J. Emery, Phys. Rev. Lett. **77**, 1342 (1996); E. Novais, E. Miranda, A. H. Castro Neto, and G. G. Cabrera, Phys. Rev. B **66**, 174409 (2002).
[24] D. M. Edwards, Adv. Phys. **51**, 1259 (2002).
[25] S. Yunoki and A. Moreo, Phys. Rev. B **58**, 6403 (1998).
[26] J. L. Alonso, J. A. Capitan, L. A. Fernandez, F. Guinea, and V. Martin-Mayor, Phys. Rev. B **64**, 054408 (2001).
[27] W. P. Su, J. R. Schrieffer, and A. J. Heeger, Phys. Rev. Lett. **42**, 1698 (1979); Phys. Rev. B **22**, 2099 (1980).
[28] T. Holstein, Ann. Phys. (N.Y.) **8**, 325 (1959); **8**, 343 (1959).
[29] J. E. Hirsch and E. Fradkin, Phys. Rev. Lett. **49**, 402 (1982); Phys. Rev. B **27**, 4302 (1983); E. Fradkin and J. E. Hirsch, *ibid.* **27**, 1680 (1983).
[30] F. D. M. Haldane, J. Phys. C **14**, 2585 (1981). For a review, see J. Voit, Rep. Prog. Phys. **57**, 977 (1994); M. Gulacsi, Philos. Mag. B **76**, 731 (1997); J. von Delft and H. Schöller, Ann. Phys. (N.Y.) **4**, 225 (1998).
[31] See, for example, V. G. Makhankov, *Soliton Phenomenology*, Mathematics and Its Applications (Soviet Series), Vol. 33 (Kluwer, Dordrecht, 1989).
[32] N. J. Curro, B. L. Young, J. Schmalian, and D. Pines, cond-mat/0402179 (unpublished).
[33] M. Gulacsi, I. P. McCulloch, A. Juozapavicius, and A. Rosengren, Phys. Rev. B **69**, 174425 (2004).
[34] C. D. Batista, J. M. Eroles, M. Avignon, and B. Alascio, Phys. Rev. B **58**, R14689 (1998); P. Horsch, J. Jaklic, and F. Mack, *ibid.* **59**, R14149 (1999); C. D. Batista, J. Eroles, M. Avignon, and B. Alascio, *ibid.* **62**, 15047 (2000); D. J. Garcia *et al.*, *ibid.* **65**, 134444 (2002); W. Koller, A. Prüll, H. G. Evertz, and W. von der Linden, *ibid.* **67**, 174418 (2003).
[35] M. Sigrist, H. Tsunetsugu, and K. Ueda, Phys. Rev. Lett. **67**, 2211 (1991); T. Yanagisawa and M. Shimoi, Int. J. Mod. Phys. B **10**, 3383 (1996).
[36] H. Tsunetsugu, M. Sigrist, and K. Ueda, Rev. Mod. Phys. **69**, 809 (1997).
[37] C. C. Yu and S. R. White, Phys. Rev. Lett. **71**, 3866 (1993).
[38] Z. Wang, X-P. Li, D-H Lee, Phys. Rev. B **47**, 11935 (1993).
[39] P. Pfeuty, Ann. Phys. (N.Y.) **57**, 79 (1970).
[40] See, for example, A. A. Abrikosov and S. I. Moukhin, J. Low Temp. Phys. **33**, 207 (1978).
[41] R. B. Griffiths, Phys. Rev. Lett. **23**, 17 (1969).
[42] D. S. Fisher, Phys. Rev. Lett. **69**, 534 (1992); Phys. Rev. B **51**, 6411 (1995).
[43] S-Q. Shen, Phys. Rev. B **53**, 14252 (1996).
[44] H. Tsunetsugu, Phys. Rev. B **55**, 3042 (1997).
[45] H. Tsunetsugu, Y. Hatsugai, K. Ueda, and M. Sigrist, Phys. Rev. B **46**, R3175 (1992).
[46] A. M. Tsvelik, Phys. Rev. Lett. **72**, 1048 (1994).
[47] S. Fujimoto and N. Kawakami, J. Phys. Soc. Jpn. **66**, 2157 (1997).
[48] K. Le Hur, Phys. Rev. B **56**, 14058 (1997).
[49] C. Lacroix, Solid State Commun. **54**, 991 (1985).
[50] M. Sigrist, H. Tsunetsugu, K. Ueda, and T. M. Rice, Phys. Rev. B **46**, 13838 (1992).
[51] P. W. Anderson, Phys. Rev. **164**, 352 (1967); P. W. Anderson and G. Yuval, Phys. Rev. Lett. **23**, 89 (1969); K. D. Schotte, Chem. Eng. Prog. **230**, 99 (1970).
[52] Y.-C. Lin, N. Kawashima, F. Igloi, and H. Rieger, Prog. Theor. Phys. Suppl. **138**, 479 (2000); D. Karevski, Y.-C. Lin, H. Rieger, N. Kawashima, and F. Igloi, Eur. Phys. J. B **20**, 267 (2001).
[53] A. J. Millis, D. K. Morr, and J. Schmalian, Phys. Rev. Lett. **87**, 167202 (2001); Phys. Rev. B **66**, 174433 (2002); T. Vojta, Phys. Rev. Lett. **90**, 107202 (2003).
[54] D. S. Fisher, Physica A **263**, 222 (1999); O. Motrunich, S.-C. Mau, D. A. Huse, and D. S. Fisher, Phys. Rev. B **61**, 1160 (2000); A. A. Middleton and D. S. Fisher, *ibid.* **65**, 134411 (2002).